The First Chaim Leib Pekeris Memorial Lecture

Ocean Tides from Newton to Pekeris

by

Sir James Lighthill

University College London

Preface by Zvi Artstein

Jerusalem 1995

The Israel Academy of Sciences and Humanities

PREFACE

by Zvi Artstein*

We have assembled here at the completion of a year since the passing of Professor Chaim Leib Pekeris, in order to honour his memory with an academic lecture. This gathering takes place under the auspices of the Israel Academy of Sciences and Humanities, of which Professor Pekeris was a leading member, and of the Weizmann Institute's Faculty of Mathematical Sciences, which he founded and headed for many years. Permit me to preface the main lecture with a number of biographical details, which, in the nature of things, will serve only as a limited sampling of the wealth of his deeds and his contributions to science, to the economy, to Israeli society and to the world.

Chaim Leib Pekeris was born in 1908 in a small town called Elytus in Lithuania to a family wth a highly-developed Jewish awareness, which passed on to its offspring a sense of responsibility for the Jewish community. Chaim was recognized as a genius already in his youth at the Kovno Hebrew Academy, and he went on to study sciences at the Massachusetts Institute of Technology, where he also excelled, of course. In a letter to a relative, he wrote (and here we may imagine his characteristic grin):

> [T]his week I received the highest mark I ever got in my life. This is my test in applied mechanics ... . The reason for the 120 is to make the mark of the majority of the students near to the passing mark.

At the same time, nineteen-year-old Pekeris was initiating activities to improve the social and economic conditions of his people in Lithuania. In a letter to a wealthy relative, Pekeris laid out a detailed plan for establishing a network of agricultural schools for Lithuanian Jews, setting forth rationales, possible sites, stages of operation and a budget. The content of the letter is revealing of the historical period:

> 90% or more of Lithuanian Jewry are not self-supporting. There are as many retail stores ... as the number of Jewish families. The government, knowing

* Professor Zvi Artstein is Dean of the Faculty of Mathematical Sciences at the Weizmann Institute of Science. The following remarks are taken from his introduction to Professor Lighthill's address at the Israel Academy of Sciences and Humanities on 22 February 1994.

> that the retail is entirely in Jewish hands, put most of the taxes on the storekeepers ... . Almost every Jew has relatives in America who support him ... . They keep on with the stores just because they have not got anything else to do.

In his habitual self-confident manner, young Pekeris continues: 'I think that if one wants to do something for the Lithuanian Jews, he should not give them what they ask, but ... establish them economically.' The solution he offers is consistent with the way of thinking that he retained throughout his life: 'They have to learn the Science of farming ... be the pioneers of modern farming in the country.'

His plan to establish agricultural schools began to take on substance, and the initial funds were budgeted, but the economic stresses of the time in America and, later, the political troubles in Europe forestalled the fulfillment of the dream. Meanwhile, Pekeris's academic career continued to thrive. He finished his bachelor's degree in 1929 and his doctorate in 1933, both at MIT, where he was supported part of the time by a prestigious Guggenheim Fellowship. After that, Pekeris was awarded a scholarship from the Rockefeller Foundation, which he used to continue his research in Boston and to spend a year at Cambridge University. From 1936 until 1941, Chaim Pekeris taught at MIT and published important articles on hydrodynamic stability, heat convection from the earth's core, and even on the role of ozone in the atmosphere. During World War II, Professor Pekeris joined the War Research Department at Columbia University in New York, where he made his contribution to the war effort through his studies on the propagation of underwater sound waves. After the war, he was appointed director of the Mathematical Physics Group at Columbia University. He published fundamental works on wave propagation in a variable substance and in the atmosphere, and on magnetic fields in different types of antennas.

During this period, the seeds of two decisive developments began to sprout. The first was Pekeris's involvement, together with John von Neumann, in the development of the electronic computer. Professor von Neumann, a refugee from Hungary and, like Pekeris, a Jewish immigrant in America, was one of the mathematical giants of the twentieth century. His interests took him into applied mathematics as well, and it was he who initiated and built the first electronic computer. After the war, von Neumann worked at IBM and later at the Institute for Advanced Study in Princeton, and it was during this period that he and Pekeris developed their strong ties of friendship and mutual esteem. Today it is hard to imagine how modern science could exist without the electronic computer, but what we now take for granted was by no means obvious in those early days. Von Neumann, and with him Pekeris, were among those who pioneered the use of the computer for research purposes, a subject to which we shall return.

Meanwhile, in New York, the first discussions about the establishment of the Weizmann Institute of Science, based on the Daniel Sieff Research Institute in Rehovot, got underway. Professor Pekeris was slated as head of one of the new institute's six departments, that of Applied Mathematics. He was an active participant in planning the Institute from both the scientific and the administrative points of view, and it is interesting to follow the course of his contributions in these matters. I shall bring just one example which typifies Pekeris's way of thinking and acting. The discussion revolved around the administrative structure of the Institute, with many of the participants arguing that the Institute should be governed by a committee composed of department heads, presided over by a director who would have the power to determine a decision only if there was no majority for any one position. Chaim Pekeris reacted to this at a meeting of the planning committee that took place at the Brooklyn Polytechnic Institute on 25 November 1946:

> ... the head of the department should be able to present his request to the director, who will be the only one whom he had to convince ... [I] do not want to spend time convincing a whole committee ... . A committee deciding on such issues would only waste time and effort ... over matters they were not in a position to evaluate adequately.

It was the opinion of Chaim Pekeris that won the day.

In 1949, Pekeris arrived in Rehovot. Along with his old acquaintance from Cambridge, Joe Gillis, with whom he worked in close cooperation throughout the long course of his career at the Weizmann Institute, Pekeris established the Department of Applied Mathematics and began to fulfill his vision of developing an advanced electronic computer in Israel. With the encouragement and help of Von Neumann, the Weizmann Institute team, led by Pekeris, improved on the Princeton computer designs and built one of the most advanced computers in the world at that time. This computer — the WEIZAC — was completed in 1955, in time to play a critcal role in several of the scientific achievements described in the following paragraphs. Today, WEIZAC is on display to the public in the entrance hall of the Ziskind Building, which houses the Faculty of Mathematical Sciences at the Institute. WEIZAC was followed by GOLEM 1 and GOLEM 2 (the latter is also on display in the Ziskind Building), and other, smaller computers for special purposes. It is difficult to overemphasize the importance of the efforts which took place in the Weizmann Institute at that time to develop the fields of computing and high-tech industries, both directly, by training experts who worked within the framework of the Institute, and indirectly, by creating conditions for the development of new frameworks, aided by the expertise of the computer personnel in the Department of Applied Mathematics.

Professor Pekeris himself continued with his theoretical and applied studies in physics and mathematics. One of his projects was the first geophysical survey of Israel, under the auspices of the oil institute that he had initiated, which concluded with the discovery of the oil field at Heletz. Only then was this operation transferred to a governmental framework, with the establishment of the Israel Geophysical Institute. Together with these endeavours in applied science and his administration of the Applied Mathematics Department (no easy matter in those days of austerity), out of which, under his leadership, grew the Faculty of Mathematical Sciences, Prof. Pekeris continued to work assiduously and in depth on the fundamental problems that confront science, making intensive use of the computers built in Rehovot. His research on the magnetic fields of the earth, on the spectroscopy of helium atoms, on the modes of free oscillations of the planet Earth and on the ebb and flow of tides made him world-famous.

Honours and prizes were not long in coming: in 1966 Pekeris was awarded the Rothschild Prize in Mathematics; in 1974 he received the very prestigious Vetlesen Prize for Earth Sciences; and in 1980 he was awarded a gold medal by the Royal Astronomical Society as well as the Israel Prize in Physics. He was appointed to many prestigious academies throughout the world, including the National Academy of Science in America, the Royal Astronomical Society, the American Philosophical Society, the American Academy of Arts and Sciences, and the Lincei National Academy in Rome; and he was of course a Member of the Israel Academy of Sciences and Humanities from 1961. Pekeris was appointed as Associate Fellow of Churchill College in Cambridge, and he received honorary doctorates from the Hebrew University of Jerusalem, Brandeis University, and Tel-Aviv University.

Alongside his scientific activities, Professor Pekeris continued to offer his advice and practical help in dealing with the social and intellectual needs of the State of Israel and the Jewish people. He was well-versed in Jewish sources, and he spent much time in the company of the noted intellectuals of the day, among them his friends Professor Gershom Scholem and the author S.Y. Agnon. He knew how to keep company with the great and powerful as well, and he corresponded with presidents and heads of governments, on more than one occasion politely rebuking them for actions or lapses of which he disapproved; and if they did not always hearken to him, they nevertheless responded with great respect. As in his youth, he took a keen interest in the situation of his people. He is well remembered for his activities on behalf of Soviet Jewry in the period when the refuseniks were victims of persecution. When Professor Alexander Lerner was left without any means to earn a livelihood in Russia, Pekeris succeeded in obtaining an appointment for him as a professor at the Weizmann Institute, on the basis of which, under Soviet law, he was able to receive financial support — also organized by Professor Pekeris. In

time, Professor Lerner was able to come to Israel, where he is engaged in active research at the Weizmann Institute to this day.

In 1973, Professor Pekeris retired and stepped down from his duties as Director of the Faculty of Mathematical Sciences, but he continued to bear the title of Distinguished Institute Professor and to be involved in every aspect of the Faculty's activities, as well as constantly moving ahead with his scientific research. The proofs of the last of his 145 scientific publications reached him only a few days before his death in a good old age, at 85.

May his memory be blessed.

The honour of delivering the first Chaim Pekeris Memorial lecture has fallen to Sir James Lighthill, who maintained a close personal and scholarly relationship with with Chaim Pekeris for many years. Sir James has served as Royal Society Professor at Imperial College, London, as Lucasian Professor of Mathematics at Cambridge University (the chair once occupied by Isaac Newton) and as Provost of University College London, where he continues to pursue his research. He is a member of the Royal Society and of many other academies around the world, and he is the recipient of numerous scientific awards and honorary degrees. He has been President of the Institute of Mathematics and its Applications in Britain, President of the International Commission on Mathematical Instruction, Chairman of the Committee on Oceanography and Fisheries of the Natural Environment Research Council, and Chairman of the Special Committee for the International Decade for Natural Disaster Reduction, established by the International Council of Scientific Unions. His ties with the Weizmann Institute, of whose Board of Governors he is an emeritus member, are long-standing.

OCEAN TIDES FROM NEWTON TO PEKERIS

by Sir James Lighthill

1. Introduction

Chaim Pekeris was one of the twentieth century's pre-eminent figures in applied mathematics, standing alongside such other giants as G.I. Taylor and Theodore von Kármán (with both of whom he closely collaborated), and his great personal friend Harold Jeffreys. Furthermore, while his contributions are of comparable importance to theirs, he seems to have exceeded even them in the extraordinary breadth of his scientific endeavours.

Pekeris's first forty years included study, research and teaching at several famous institutions: at MIT before the Second World War (with a sabbatical absence at Cambridge University, during which he first met Taylor and Jeffreys), at Columbia University during the war years, and at Princeton's Institute of Advanced Study immediately afterwards. Then the twenty-five year period from 1949 to 1973 saw Pekeris dedicatedly engaged in Israel. As inaugural Head of the Department of Applied Mathematics, he created a great centre in what I like to call 'the art of applying mathematics' — and also devoted much attention to 'the art of teaching the art of applying mathematics.' Simultaneously, he developed geophysical prospecting (including gravimetric survey) for Israel, to the great benefit of the country's natural resources, and established the Geophysical Institute. Meanwhile, at Rehovot, he successively developed WEIZAC and GOLEM as a superb sequence of computers for giving still greater power to creative applied mathematicians. Above all, he inspired the young at the Weizmann Institute with a characteristic combination of roguish humour and brilliant scientific and mathematical insight. Then, in his last twenty years, Emeritus Professor Pekeris simply went on and on to yet further fields of study on the Rehovot campus, while becoming the recipient of innumerable honours in the United States, Israel and Europe.

The vast range of scientific fields illuminated by Pekeris might conveniently be grouped under six major headings: (i) atomic physics, a field in which Pekeris is honoured as the one who, in a series of papers, 'got helium right' — he also did lithium; (ii) microwave propagation and associated antenna theory, to which he was introduced by his wartime researches; (iii) seismology, a field into which he was drawn by his friendship with Harold Jeffreys, with enormous benefits to geophysical work in Israel; (iv) other aspects of the mechanics of solids with geophysical applications (including studies of free oscillations of the Earth,

alongside a related field that he called 'terrestrial spectroscopy': using such studies to interpret spectra of relevant instrumental data); (v) fluid mechanics, including ocean tides and atmospheric tides (another tidal topic, the 'bodily tide' in the solid earth, falls within field [iv]); and, lastly, (vi) general relativity — a field into which he moved after his retirement!

As a specialist in fluid mechanics, I am tempted to suggest that this field contains particularly large areas which Pekeris illuminated. Apart from ocean tides, which I shall discuss here in detail, he worked extensively on the propagation of sound and shock waves, both in the atmosphere and in the ocean — another subject to which he was introduced by wartime researches. He also made contributions of fundamental importance to nonlinear features of the instability of fluid motions, and to that theory's relationships with transition to turbulence. In addition, he illuminated several aspects of the relationships of fluid mechanics to more general physical science — for example, atmospheric ozone, astrophysical oscillations, and the kinetic theory of gases.

In all this wide-ranging scientific activity, Pekeris's work on ocean tides forms just a small fraction of his total output, but his six papers on that subject were of especial excellence. One of them, moreover, his 1969 paper with Y. Accad, 'Solution of Laplace's equations for the M_2 tide in the world oceans,' was of a revolutionary importance which I regard as fully justifying the title of this paper.

2. Introductory Remarks about Sound Waves

I shall devote three sections to introductory remarks about waves, such as those which I am using to send messages to your ears. A sound wave in air travels at a speed c, whose square was shown by Newton (1686) to be equal to the ratio of pressure changes to density changes in a sound wave:

$$c^2 = \frac{dp}{d\rho} . \tag{1}$$

This conclusion may be understood relatively simply from a one-dimensional diagram (Diagram 1a) showing a wave propagated in just one direction, the x-direction. The diagram plots against x some quantity q (which may be the pressure p, or the density ρ, or the air velocity v), and the solid line indicates the 'wavy' way in which q varies with x at a particular instant. Then the broken line shows this wavy form of variation (the 'waveform') after it has moved on a distance dx during a time interval

$$\frac{dx}{c} . \tag{2}$$

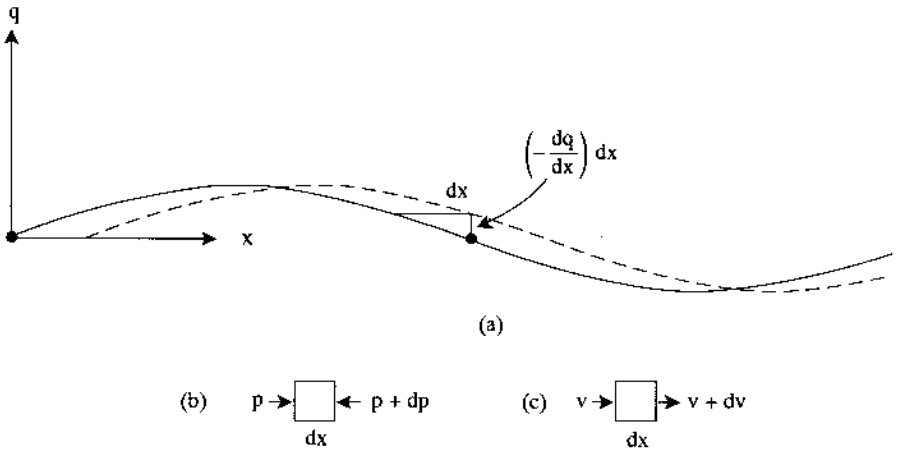

Diagram 1 (a) One-dimensional propagation of a wave in the x-direction. The solid line plots the quantity q against x at a certain instant, and the broken line shows this plot after the wave has moved on a distance dx. Expression (4) gives the change in q between the solid and the broken line — which, on division by the time interval (2), yields the rate of change (3).
(b) Expression (7) gives the force acting in the x-direction per unit volume of fluid.
(c) Expression (10) gives the compression rate per unit volume of fluid.

Often I shall use the result that the rate of change with time of any quantity q in a wave is

$$-c\frac{dq}{dx}\,. \tag{3}$$

Thus, it is positive at any point — like the point picked out in the diagram with an arrow — where q has a negative (that is, downward) gradient. At such a point, q increases between the solid and broken lines by the amount

$$\left(-\frac{dq}{dx}\right)dx\,, \tag{4}$$

and division of this change by the time interval (2) gives the expression (3) for rate of change.

For example, if we take q to be the air velocity v, we obtain its acceleration (rate of change of v) as

$$-c\frac{dv}{dx}\,. \tag{5}$$

Now, Newton's Second Law of Motion (Newton 1686) states that mass times acceleration equals force. Applied per unit volume of air, it gives

$$\rho\left(-c\frac{dv}{dx}\right) = -\frac{dp}{dx}, \tag{6}$$

where mass per unit volume is the density ρ, acceleration takes the form (5), and Diagram 1b explains why the force per unit volume acting in the x-direction is

$$-\frac{dp}{dx}. \tag{7}$$

From equation (6) follows the important expression

$$\rho c v \tag{8}$$

for excess pressure.

Again, if we take q to be the density ρ itself, we can write down an equation

$$-c\frac{d\rho}{dx} = \rho\left(-\frac{dv}{dx}\right) \tag{9}$$

which puts the rate of change of density equal to the density ρ itself multiplied by the compression rate

$$-\frac{dv}{dx}. \tag{10}$$

Diagram 1c explains this form (10) for the compression rate (more precisely, it explains how the air between a position x, where the velocity is v, and a position $x+dx$, where it is $v+dv$, has an expansion rate per unit volume equal to a ratio of dv to dx; the compression rate taking, therefore, the same value with the sign changed).

From equation (9) a form

$$\frac{\rho v}{c} \tag{11}$$

for the excess density is deduced. With equation (8) for excess pressure, this yields Newton's expression (1) for c^2 as the ratio of excess pressure to excess density.

3. Introductory Remarks about Shallow-Water Waves

After our discussion of sound waves, it is interesting to ask whether there are any water waves whose propagation in one dimension is of an essentially similar nature. It turns out that this is indeed the case for 'waves in shallow water'. The meaning of this expression is that the depth h is small, not in any absolute sense, but in

comparison with the wavelength (the distance within which the waveform of Diagram 1a repeats itself).

For waves in shallow water, any increase of depth h produces an excess pressure equal to ρg times the excess depth. Here, ρg is the weight of water per unit volume (whose ratio to the mass ρ per unit volume is g, the gravitational acceleration). Then Newton's Second Law (6), expressed now per unit volume of water, becomes:

$$\rho\left(-c\frac{dv}{dx}\right) = -\rho g\frac{dh}{dx} \tag{12}$$

so that excess depth can be expressed as:

$$\frac{cv}{g}. \tag{13}$$

Again, the rate of change of depth can be written according to the general principle (3) as:

$$-c\frac{dh}{dx} = h\left(-\frac{dv}{dx}\right) \tag{14}$$

where the right-hand side represents the depth h multiplied by the compression rate (10); thus, although the water remains effectively incompressible, horizontal compression is able to be accompanied by an increase in water depth without change of density.

From equation (14) a form

$$\frac{hv}{c} \tag{15}$$

for the excess depth is obtained (analogous to the form (11) for the excess density). With expression (9) for the same quantity, this yields a classic equation:

$$c^2 = gh \tag{16}$$

for the speed c of one-dimensional propagation of waves in shallow water of depth h.

Actually, the analogy with sound-wave propagation is rather complete. Thus, if we take the view that an 'effective' excess density is:

$$\frac{\rho}{h}\ \text{(excess depth), while excess pressure} = \rho g\ \text{(excess depth)}, \tag{17}$$

then Newton's value for c^2 as excess pressure divided by excess density takes the 'effective' value (16) for shallow-water waves.

4. Numerical Values of Shallow-Water Wave Speed

Values of the shallow-water wave speed c, given by equation (16) for various depths h, are tabulated below:

	Depth h (metres)	$c = \sqrt{(gh)}$ (m/s)	$\frac{c}{g}$ (seconds)
Estuaries	1	3	0.3
	10	10	1
Continental shelf	40	20	2
	100	30	3
Deep oceans	1000	100	10
	4000	200	20
	10000	300	30

It is noteworthy that the values of c characteristic of deep oceans have magnitudes which approach that of the speed of sound in air (340 m/s). But we need to ask whether the theory of Section 3 can really be applied to deep oceans.

Essentially, the theory is one which concentrates upon v, the horizontal velocity of the water, while neglecting any dynamic effects of vertical motions. Now these have a typical speed

$$\frac{dh}{dt}, \tag{18}$$

the rate of increase of water depth (where t is time). With expression (13) for the excess depth, this rate of increase (18) has an order of magnitude:

$$\frac{cv}{gT}, \tag{19}$$

where T is the wave period. Thus, the condition for vertical velocities to be negligibly small compared with v, so that the theory of Section 3 can be applied, is that the period T must be much greater than the quantity

$$\frac{c}{g}, \tag{20}$$

values of which are given in the above table.

Evidently this condition is satisfied, with an enormous margin to spare, for ocean tides, which have periods of at least 12 hours, while the quantity (20) never exceeds about half a minute. By contrast, ordinary waves on the sea surface have periods of around 5 to 10 seconds and fail to satisfy the conditions; in other words, vertical motions are important for such surface waves.

For tides, on the other hand, we can expect equation (16) to apply even in deep oceans. Actually, the average depth of the world's oceans is 4 km, for which c = 200 m/s (see Table). At this speed, a wave would travel about 4000 km in 6 hours (about half a tidal period), suggesting that distances between 'nodes' (places where the waveform crosses the x-axis — see Diagram 1) might be around 4000 km.

5. Tides Viewed as Shallow-Water Waves

There is a suggestion here that 'deep oceans masquerade as shallow water' for propagation of tidal motions. Furthermore, these are primarily horizontal motions.

Indeed, even though tides seem superficially to be periodic vertical motions that alter sea level, essentially all their kinetic energy is in the horizontal motions. It appears in that pattern of powerful tidal currents which offers exciting spectacles off many coastlines. At a headland, for example, the current may be observed rushing past from left to right, while six hours later it is seen to be rushing with equal vigour from right to left!

Essentially, the pattern of such tidal currents is propagated in a wavelike manner. The type of wave propagation involved, moreover, is that characteristic of shallow-water waves.

6. Newton's Elucidation of Tide-raising Forces

Newton (1686) recognized that his gravitational theory explained why the moon has a very special influence on tides. Diagram 2 (below) gives a schematic illustration of his ideas on the subject. It depicts the effect of an attracting body — which might be the moon (or, alternatively, the sun) — both on the solid earth and on the oceans.

If the solid earth could be viewed essentially as a rigid body, Newton showed that its motion would be that generated by the value of the gravitational force exerted by the attracting body at the earth's centre. At the same time, because Newton's universal law of gravitation requires the gravitational force to decrease (according to an inverse-square law) with distance from the attracting body, different parts of the ocean would be subject to different forces:

(i) water nearest to the attracting body would be subject to a greater gravitational force; in other words, to an excess attraction over that experienced by the solid earth; while

(ii) water farthest from the attracting body would experience a deficit in gravitational force; in other words, a relative repulsion (relative, that is, to the solid earth's own motion).

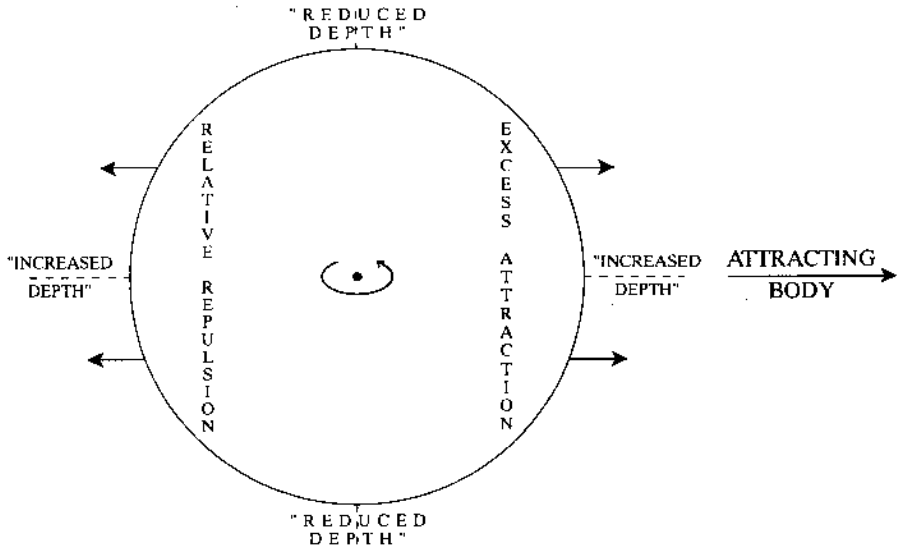

Diagram 2 Gravitational forces tending to raise sea level (short arrows) reach maxima at points nearest to and farthest from an attracting body. They are known as tide-raising forces. As explained in Section 7, Newton considered that the resulting ocean depth distributions might be as suggested schematically by the broken lines. Later (Section 8), Laplace noted that the horizontal components of the forces play leading roles, being able moreover to produce a convergence of tidal currents that would raise sea level.

For any attracting body, then, forces tending to raise sea-level (known as tide-raising forces) would reach maximum values at points on the earth's surface nearest to and farthest from the attracting body. However, because the earth is rotating, the positions of these locations of maximum tide-raising force would vary, with periods close to 12 hours.

Does the moon or the sun exert the greater tide-raising forces? Of course the sun is enormously more massive than the moon, but it is also very much farther away. Now, Diagram 2 shows that tide-raising forces depend not on the absolute value of the gravitational attraction (which is greater for the sun), but on the difference between values of that attraction on the two sides of the earth. It depends, in other words, on the gradient of gravitational force with distance from the attracting body. Newton showed how this is about 4.5 times greater for the moon than for the sun.

The largest tide-raising forces, then, are experienced at points nearest to and farthest from the moon. But they are augmented still more if and when these points

almost coincide with the points nearest to and farthest from the sun. Then the moon's tide-raising force is augmented by an approximately collinear solar force.

Such an approximate collinearity occurs once a fortnight, at full or new moon (for example, when seen from the earth as fully illuminated by the sun, the moon must be nearly in line with sun and earth), and produces the relatively stronger 'spring' tides. By contrast, rather weaker 'neap' tides appear halfway between the full and the new moon (when the two tide-raising forces are orthogonal).

Etymologically, the word 'spring' in 'spring tides' possesses a different Germanic root from 'spring' in the sense of season, and lacks any seasonal connotation. However, the well-known tilt in the earth's axis of rotation means that the approximate collinearity of sun and moon occurring once a fortnight becomes a near-perfect collinearity at an equinox (either March or September). So the equinoctial spring tides tend to be stronger still; by contrast, equinoctial neap tides are even weaker than ordinary ones!

7. What Tides Arise from Tide-Raising Forces?

Diagram 2 illustrates schematically not only the tide-raising forces identified by Newton, but also Newton's tentative ideas about the changes in sea-level that they would produce. Essentially, he expected high tides to occur at those locations on the rotating earth where tide-raising forces are greatest. But the problems of determining what real ocean tides arise from tide-raising forces are much more difficult, for a reason that has been indicated in Section 5 and for other reasons.

Before embarking on this subject, however, I'll briefly mention two other tidal themes that greatly interested Pekeris. Essentially, the same tide-raising forces act on the atmosphere. Thus, the problem of atmospheric tides, to which Pekeris was introduced by G.I. Taylor, is one of identifying the atmosphere's own response to tide-raising forces. A further issue, brought to his attention by Harold Jeffreys, is that of the earth's bodily tide, upon which we shall touch again later. It arises from the deformability of the earth, which allows the tide-raising forces of Diagram 2 to produce departures from the 'rigid-body' motions there assumed for the solid earth as a whole. There are intricate difficulties involved in investigating these departures, but we shall leave them aside in the present context.

8. Laplace's New Look at Ocean Tides

It was Laplace (1775), at the age of 26, who initiated and used a highly impressive fluid-mechanical analysis to give a picture differing from that of Newton in three important aspects:

(i) it allowed for the essentially wavelike character (Section 5) of the pattern of ocean-current response to tide-raising forces; of which, furthermore,
(ii) only the horizontal components could energize tidal currents (sea-level then being raised, as explained in the caption to Diagram 2, by the convergence of those horizontal currents); while, moreover,
(iii) the earth's rotation, besides determining periods for different tide-raising forces, also has an important dynamic effect.

I shall concentrate here on describing the essential physics associated with Laplace's analysis; moreover, just as conclusion (i) has already been explained in Sections 2 through 5 by comparing one-dimensional propagation of sound and shallow-water waves and showing them to be essentially similar, so also the new and important conclusion (iii) will be explained in Sections 9 through 12 by comparing two-dimensional propagation in the two cases. (Evidently, the two dimensions with which we are concerned in relation to propagation of tidal currents are the north-south and the east-west dimensions.) This time we shall find that an important difference emerges.

9. Sound Waves in Two Dimensions

Air motions in any sound wave constitute a 'potential' field, that is, one that may be derived from a scalar potential — as an electric field is from an electric potential or a magnetic field from a magnetic potential. In fluid-mechanical terms, this means a field without vorticity.

The physical interpretation of this important conclusion emerges most simply if we consider the dynamics of a small sphere of fluid (Diagram 3). The forces acting on such a sphere are all pressure forces acting at right angles to its surface. These pressure forces are not necessarily equal all around the boundary; however, they all act through its centre, and therefore cannot alter its angular momentum.

Now, vorticity (see Section 10) specifies the angular momentum of such a small sphere; which, if it is initially zero, must remain zero. It was another great French applied mathematician, Lagrange, who first enunciated this important result — that when a fluid motion has zero vorticity everywhere at one moment, then the vorticity will continue to be everywhere zero.

This is important for sound waves, because when they propagate through air that is previously undisturbed (and therefore has zero vorticity), the air motions will continue to have zero vorticity. In two dimensions, for example, this means that any 'shears' in the x- and y-components of the air velocity, u and v, must make cancelling contributions to the angular momentum (Diagram 3). This is the condition

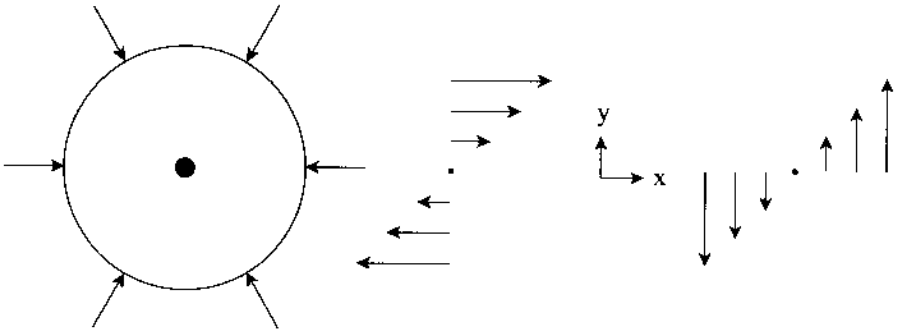

(a) (b)

Diagram 3 (a) Because pressure forces acting on a small sphere of fluid are directed through its centre, they do not change its angular momentum. If this angular momentum is initially zero (in a sound wave, for example), it will remain zero.
(b) In a two-dimensional sound wave, shears can be present only if (as in the case shown) equation (21) is satisfied — giving them cancelling (clockwise and anticlockwise) contributions to angular momentum.

$$\frac{\partial v}{\partial x} = \frac{\partial u}{\partial y}\,, \tag{21}$$

which is automatically satisfied in any 'potential' field with u and v as the x- and y-derivatives of a potential.

10. Further Explanations about Vorticity

It may be desirable to explain this behaviour of sound a little further, in preparation for appreciating the different behaviour of shallow-water waves. The explanation continues to be based on the dynamics of a small sphere of fluid.

Such a sphere's motion can be divided into three parts (Diagram 4, below):

(i) uniform translation with the velocity of the centre;
(ii) rigid rotation with angular velocity $\frac{1}{2}\omega$ (where ω is the vorticity); and
(iii) a symmetrical squeezing or 'straining' motion.

Evidently, parts (i) and (ii) are motions of which a rigid body would be capable; and they carry, respectively, all of the sphere's linear and all of its angular momentum. But a fluid sphere, far from being rigid, is of course highly deformable, and part (iii) represents its instantaneous rate of deformation or 'strain', usually involving an

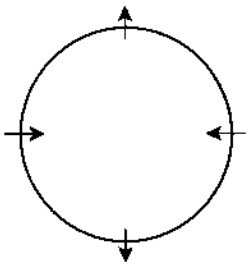

Diagram 4 The general motion of a small sphere of fluid consists of a simple rigid-body motion, made up of a translation (i) and a rotation (ii), in combination with a deformation (iii) that takes the form of a symmetrical straining motion as shown here.

elongation in one direction and a foreshortening in some direction at right angles.

It is worth recalling (Diagram 5) that a simple rigid rotation with angular velocity ω involves at a distance r from the centre of rotation a motion with velocity ωr, which can be resolved into x- and y-components as shown (the x-component u being $-\omega y$ and the y-component v being $+\omega x$). Thus, the rotation is a combination of two shears — each of which separately must have angular velocity $\frac{1}{2}\omega$ in its own separate 'part (ii)' motion, so that its vorticity is ω. Moreover, the fact that each of the two shears depicted in Diagram 5 possesses on its own the vorticity ω permits us to write the vorticity ω for a quite general two-dimensional motion as

$$\omega = \frac{\partial v}{\partial x} - \frac{\partial u}{\partial y}\,; \tag{22}$$

obtained, of course, from adding up the contributions to ω from local shears in the x-component u and in the y-component v of fluid velocity.

As indicated in Diagram 4, part (iii) of the sphere's motion may involve an elongation in one direction. In the propagation of shallow-water waves, for

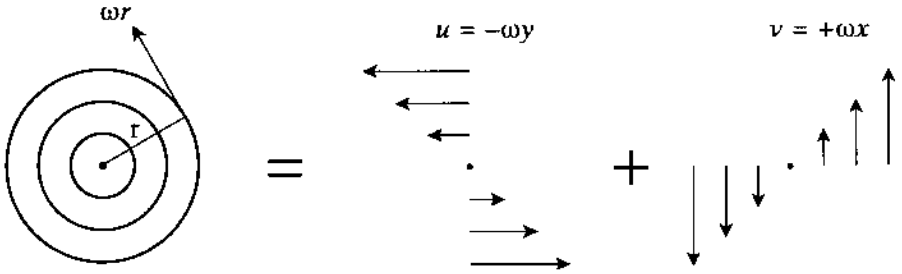

Diagram 5 A simple rigid rotation with angular velocity ω creates at a distance r from the centre a motion with velocity ωr, which can be resolved into x- and y-components as shown. It follows that each of these shearing motions has vorticity ω.

example, this may be the vertical direction wherever there is an increase of water depth h from its initial value h_0. Such an elongation, necessarily accompanied by foreshortening in a direction at right angles, reduces the moment of inertia about the axis which is being elongated. Therefore, since the sphere's angular momentum is not changing (Section 9), its angular velocity about this axis must be increasing. (We see this when an ice skater, in the course of a spin, raises her arms above her head, decreasing her moment of inertia about a vertical axis and thus increasing angular velocity.) These effects augment the vorticity ω by just that factor

$$\frac{h}{h_0} \tag{23}$$

by which the sphere is being vertically elongated.

11. Shallow-Water Waves in Two Dimensions

It is at first not at all obvious why the augmentation factor (23), which in shallow-water wave propagation must be applied to the vorticity, should be of any significance. Indeed we can still conclude as in Section 9 that, if the vorticity is zero initially, then it must remain zero, producing the same equation (21) that is satisfied by sound waves.

But the earth rotates at an angular velocity of one revolution (or 360°, or 2π radians) per day. Thus, every small sphere of water in the ocean shares this angular velocity of 2π radians/day, so that part (ii) of its motions (see Section 10) possesses an initial vorticity — before the shallow-water waves appear — equal to 4π/day.

Actually, we are only interested in the vertical component of vorticity, because this is the component which is stretched by any increase in sea level and also because horizontal motions are associated by equation (22) with a vertical component of vorticity. At the North Pole, where the latitude θ is 90°, the vertical vorticity takes the full value of 4π/day, but at any other latitude the vorticity due to the earth's rotation has to be multiplied by $\sin\theta$ to give its vertical component as

$$f = \frac{4\pi \sin\theta}{\text{day}} = \frac{4\pi \sin\theta}{24(3600)\text{s}} = (1.45 \times 10^{-4} \sin\theta)\text{s}^{-1}. \tag{24}$$

This very famous quantity f is now usually called the planetary vorticity.

In shallow-water waves, then, the water's initial vorticity before the waves appear takes the value f. This is then augmented by the factor (23) wherever ocean depth h is increased above its initial value h_0.

Out of this augmented vorticity, of course, the part f still corresponds to the earth's rotation, so that it is the remaining part,

$$f\left(\frac{h}{h_0}-1\right), \tag{25}$$

which must correspond to effects other than the earth's rotation. These are the effects (22) of shears in the water's horizontal motions.

12. The Physics of Tidal Currents

Now I am able to summarise briefly the essential physics underlying the behaviour of tidal currents. Their propagation, as shallow-water waves in two dimensions, is very much like that of sound waves (the wave velocity c being, however, related as in equation (16) to the local water depth), except that the vorticity is not zero. In fact, the value of the vorticity (22) is dominated by the expression (25) associated with vertical stretching of planetary vorticity.

Actually, the expression for the vorticity (22) also includes another term — though this is generally a lot smaller. Any small northward displacement n of a fluid sphere causes the planetary vorticity (24) to increase by βn (the 'beta effect'), where

$$\beta = (2.3 \times 10^{-11} \cos\theta)\mathrm{s}^{-1}\mathrm{m}^{-1} \tag{26}$$

The sphere's total vorticity can then be written $(f + \beta n) + \omega$; and, equating this to the initial value f multiplied by the stretching factor (23), we obtain

$$\frac{\partial v}{\partial x} - \frac{\partial u}{\partial y} = \omega = -\beta n + f\left(\frac{h}{h_0}-1\right) \tag{27}$$

as a (generally moderate) correction to expression (25).

I have tried to outline only the essential physics underlying the behaviour of tidal currents. Laplace (1775) derived the corresponding full equations of motion in a rigorous mathematical way, and they are necessarily quite complicated in their detailed forms; in particular, they need to use latitude and longitude as coordinates (that is, not Cartesian coordinates x and y such as were adopted in Sections 9 through 11, but spherical polar coordinates). They represent, of course, an enormous step forward from Newton's ideas of tides (Diagram 2); and it is, perhaps, not surprising that almost a century separated the work of Newton (1686) from that of Laplace (1775).

Against this background, it may, however, seem quite surprising that Laplace's

tidal equations were not actually solved for any realistic ocean until almost two centuries later. This was the very special achievement of Pekeris & Accad (1969), which is described in Sections 15 through 17. Before it, the only use made of Laplace's tidal equations had been to derive solutions for extremely simple model problems with highly arbitrary and unrealistic geometries. (For an excellent compendium of pre-Pekeris knowledge on tides, see Defant [1961].) It is thus no exaggeration to view the three principal milestones in the mathematical analysis of tides as having been the investigations of Newton, Laplace and Pekeris. But I must lead you back once more to the work of the first of these great scientists before trying to describe the successes of the third.

13. The Spectroscopy of Tides

Absolutely all mathematical analyses of tides, and all interpretations of tidal observations, start from Newton's elucidation of tide-raising forces (Section 6) and spectrally analyse them. The largest component is known as M_2, the moon's 'semi-diurnal' influence; actually, its period T is longer than half a day by one twenty-eighth (giving $T = 12$ hours 25 minutes), because the moon's orbital motion is in the same sense as the earth's rotation but has a period 28 times greater.

The next-largest component of the tide-raising forces is known as S_2: that part of the sun's tide-raising force which has period T almost exactly equal to 12 hours. There are very many other spectral components (practically all with much longer periods) which I do not need to define here, observing in particular that the basic cycle (Section 6) of spring tides and neap tides derives from the 'beats' between M_2 and S_2.

For constructing tide tables, of course, very many different components in the spectrum of tide-raising forces must be taken into account. Then, for example, corresponding spectral components in the data gathered from tide gauges need to be identified, and utilised in the prediction of tidal behaviour. This work is of the greatest practical importance; in itself, however, it fails to probe those physical mechanisms by which (say) the M_2 tide-raising force produces the M_2 tide.

14. Tides Near Shorelines

One of these physical mechanisms has not yet been mentioned, because Laplace (1775) did not allow for it, although Pekeris & Accad (1969) did take it into account. It is associated with the behaviour of tides near shorelines.

On any continental shelf, tidal kinetic energy becomes relatively concentrated within the relatively shallower water near a shoreline. This causes tidal currents to

be augmented, leading to significant dissipation of energy by bottom friction in these shallower waters. What is the energy source that compensates for such dissipation?

The energy source for the tides is the earth's rotation itself (which stores energy rather as a flywheel does in some machines). If the earth rotated so slowly as to turn always the same face to the moon, then there would be no M_2 tide, or any other tidal movements of lunar origin. The effect of the moon in this case would be to produce (as in Diagram 2) a static elevation of water at the points nearest to and farthest from the moon itself.

Tidal movements of lunar origin, then, are due to excess rotation (i.e., to the fact that the day is shorter than the moon's orbital period) and derive their energy from it. Accordingly, dissipation of such energy reduces that excess; in other words, 'tidal friction lengthens the day'! (Simultaneously, it reduces the moon's orbital period, since the overall angular momentum of the earth–moon system cannot be changing; clearly, this effect conspires with the lengthening of the day to diminish further the difference between the day and the moon's orbital period.) It was G.I. Taylor (1919) who first verified the above statement through estimates of the rate of dissipation of tidal energy in shallow seas. The average lengthening of the day that results is by about a millisecond per century.

Before proceeding in Section 15 to consequences of the fact that ocean tides represent a damped system of forced oscillations of the world's oceans in response to tide-raising forces, I'll end this section by asking a simple question, not explicitly related to ocean tides as such. Why is it that the moon always turns the same face to us? The answer is that the process described above, whereby dissipation of tidal energy progressively reduces differences between the earth's period of rotation and the moon's orbital period, was long ago carried through to completion as far as the bodily tides in the much smaller moon were concerned. Dissipation of their energy reduced the difference between the moon's period of rotation and its orbital period until the present very familiar situation was reached, in which both are identical.

15. Numerical Analysis by Pekeris & Accad

Pekeris and Accad (1969), boldly taking up the scientific challenge, used the then relatively new GOLEM computer to obtain, for the first time, a solution of the tidal equations of Laplace (1775) for a realistic ocean model. The one feature they added to the original form of Laplace's equations (for reasons outlined in Section 14) was a representation of frictional forces resisting tidal currents near shorelines. They then pursued the objective of computing the M_2 tide (see Section 13) in the world's oceans, using refined numerical analysis to achieve this goal.

Covering the oceans with a grid of points separated by 1° spacings in both latitude and longitude, they needed to solve a linear system of simultaneous equations with 50,000 unknowns; namely, the amplitude and phase of each component of velocity (the eastward component u and the northward component v) at each grid point. They carried out the computations both for the real system — the damped forced oscillation in which bottom friction near coasts plays a significant role — and for the original undamped forced oscillation described by the unmodified tidal equations of Laplace.

Interestingly, the numerical analysis in the case where allowance was made for friction exhibited two important features to an enormously greater degree than when the undamped system was treated. These features were:

(a) stability (of the solution as the grid spacing was reduced, say from 2° to 1°); and
(b) insensitivity (to details of the assumed coastline shapes).

All of the computations carried out by Pekeris & Accad (1969) that incorporated frictional damping possessed qualities (a) and (b) to a most satisfactory degree.

16. The M_2 Tide as Depicted by Pekeris & Accad

The ocean model with 1° grid spacing which Pekeris & Accad (1969) used is reproduced in Figure 1.* Coastlines are composed of meridians of longitude and parallels of latitude, arranged for convenient use with a 1° grid spacing (those for Europe and Asia, moreover, being drawn as continuous across the Straits of Gibraltar, since these are penetrated by negligible amounts of tidal energy). The contour lines for ocean depths are given in metres at intervals of 500 m, and represent a 'smoothed' variation of depth for the world oceans.

Figure 2 represents the M_2 tide computed for this model ocean with 1° grid spacing, taking bottom friction into account. Here, the broken lines are 'co-range lines'; that is, they are contours of the tidal range in metres. (The tidal range, of course, is the vertical distance between high and low tide; thus, the vertical amplitude of the M_2 tide takes a constant value along any one of these broken lines.) The solid lines are 'co-tidal lines'. All along any of these solid lines high tide occurs at one and the same time. This makes them contours of the phase of high tide, which is specified in 'hours' relative to the time of lunar transit across the Greenwich meridian. (Strictly, these 'hours' are lunar hours, defined as one-twelfth of the M_2 tide's basic period of 12 hours and 25 minutes.)

Extremely striking features of such a map are the amphidromes. These are points

* The Figures are reproduced consecutively at the end of this brochure.

where values of the tidal range become zero while values of the phase 'rotate' around them. In terms of the physics of tidal currents (Section 12), the spacing of amphidromes in Figure 2 may be related to the propagation properties of shallow-water waves. In a 'waves' context these points where the range becomes zero may be regarded as 'nodes', expected (see the end of Section 4) to have average spacings of around 4000 km — an expectation broadly supported by Figure 2. At the same time, the essential contribution made by vorticity to the physics of tidal currents is reflected in the phase 'rotation' around each amphidrome.

Although the existence and importance of amphidromes had long been recognized, it was the work of Pekeris and Accad (1969) that established how widely they are distributed. For example, the existence of a South Atlantic Amphidrome had not previously been suspected; accordingly, the authors treated their prediction of this prominent new amphidrome as a test case, triumphantly demonstrating (Section 17) how well their South Atlantic predictions agreed with observation.

17. Some Tests of the Computed Results

But their first, absolutely essential tests of the computed results concentrated on those two specially important features of the numerical analysis which I designated as (a) and (b) in Section 15. For example, Figures 3 and 4, when compared with each other and with Figure 2, demonstrate rather clearly the 'stability' feature (a). In Figure 3, coastlines are approximated more crudely, for convenient use with a 2° grid spacing. Plotting the results of computations with that spacing, it obtains co-range and co-tidal lines not very different from those of Figure 2. Again, their comparison with Figure 4, a computation using a 1° grid spacing but the same cruder coastline shapes as Figure 3, shows similarly good agreement. Other comparisons, involving rather larger variations of coastline shape, also confirm the 'insensitivity' feature (b).

As for their demonstration of the validity of their discovery of the South Atlantic Amphidrome, Figure 5 shows how Pekeris & Accad (1969) made detailed comparisons of their predictions in the South Atlantic with observations at relevant islands, including Ascension, St. Helena, Tristan da Cunha and South Georgia. At each such island the observed phase in 'hours' (see Section 16) is underlined, while the observed range, this time in centimetres, is bracketed. These observations correspond fairly well to the computed results and are seen to establish very clearly the existence of this important amphidrome.

Generally, the computations of Pekeris and Accad (1969) give quite good agreement with observations in the Atlantic and Indian Oceans. There are, however,

a few parts of the Pacific where agreement is poor; and the fact that these parts include the general vicinity of the distinguished Scripps Institute of Oceanography in La Jolla, California, may have influenced 'Scripps-oriented' oceanographers to undervalue the marvellous breakthrough in tidal knowledge which the 1969 paper represented!

18. Further Advances in the Next Nine Years

I'll mention just one more paper, published by Accad & Pekeris (1978) nine years later. This was important in several different ways. Above all, it calculated the S_2 tide as well as the M_2 tide. Though this was an extremely valuable addition, in the present framework I discuss only their new results on the M_2 tide.

The 1978 paper allowed for two 'secondary' effects in addition to those taken into account in the 1969 paper. First, it allowed for tidal yielding of the solid earth — including deformations both in response to the tide-raising forces themselves and in response to tidal shifts in the weight of ocean water overlying the solid bottom. Secondly, it allowed for the water's gravitational self-attraction. Neither of these effects was expected to be very significant, and they were found in combination to yield a correction of only about 10%, but Accad & Pekeris (1978) rightly emphasized how important it had been to establish quantitatively the size of that correction. Moreover, this modest correction proved to be particularly important in its influence on the placing of the Northeast Pacific Amphidrome. Instead of being placed erroneously almost on the Californian coast, as in Figures 2, 3 and 4 above, the correction shifted it offshore to a position fully consistent with observations at La Jolla and elsewhere on that famous coastline.

In addition, Accad & Pekeris (1978) introduced an improved representation of bottom friction near shorelines, which they referred to as the sloping-shelf model. With this representation they obtained not only the previous benefits of features (a) and (b) as described in Section 16 but also excellent agreement with observations in practically all parts of the world's oceans.

19. The M_2 Tide as Described by Accad & Pekeris (1978)

By 1978 a more detailed distribution of ocean depth, shown in Figure 6 on a 1° grid representation, had become available to Accad and Pekeris. However, they applied it exclusively in a smoothed version using a 2° grid, because of the 'stability' property (a) which they had previously established. Figure 7 shows their computation of the M_2 tide as thus obtained, allowing for the effects noted in Section 18.

Here the good agreement with observations in the Atlantic and Indian Oceans became still better. The greatest improvement, however, was in the Northeast Pacific, where the movement of the amphidrome away from the Californian coast produced the correct northward progression of high tide along that coast. Figure 8 shows this area in an enlarged form with observed data included.

Another comparison with observations along the Northeast Pacific coast is given in Figure 9. Observed phases are extremely close to the computed curve; observed ranges, however, are a little higher than the computed values because the 2° grid does not sufficiently resolve the near-shore regions of shallower water.

Similarly good comparisons are found for the West Atlantic coast in Figure 10. As to the Western Pacific, where the 2° grid (Figure 7) effectively makes an impermeable barrier out of East Asia and Australasia, Figure 11 again shows excellent agreement between computations and tidal observations from Sydney to Kamchatka — with, perhaps, the single exception of the Coral Sea, where the assumption of impermeability is least realistic.

Accad & Pekeris (1978) also showed that proper boundary conditions for their model could satisfactorily be applied even at smoothly shaped ocean boundaries. Figure 12 shows the results of this computation, with all other aspects of the model the same as in Figure 7. The data are extremely close to the results shown in Figure 7. At the same time, this final representation of the computed M_2 tide may perhaps be the most useful of all from a broad geophysical standpoint.

20. Ocean Tides from Newton to Pekeris

What an enormous difference we observe between this modern picture of tides in the world oceans and those simple ideas, schematically illustrated in Diagram 2, that were originally put forward by Newton! Newton's elucidation of tide-raising forces has of course continued to be recognized as essentially correct (Section 13), but his over-simplified view of the ocean tides that those forces generate stands in the sharpest possible contrast to the complex picture delineated in Figure 12.

But then we may perhaps recall Newton's own famously modest comparison of his labours to 'playing on the seashore' while 'the immense ocean of truth extended before me unexplored.' It was above all the initiative of Chaim Pekeris that mapped the immense ocean of tidal truth.

References

Accad Y. & C.L. Pekeris (1978) 'Solution of the Tidal Equations for the M_2 and S_2 Tides in the World Oceans from a Knowledge of the Tidal Potential Alone', *Phil. Trans. Roy. Soc., A* 290 : 235–266.

Defant A. (1961) *Physical Oceanography*, I–II, Oxford.

Laplace P.S. (1775) *Mém. Math. Phys. Acad. Roy. Sci.* (Paris), pp. 75–182.

Newton I. (1686) *Philosophiae Naturalis Principia Mathematica*, I–III, London.

Pekeris C.L. & Y. Accad (1969) 'Solution of Laplace's Equations for the M_2 Tide in the World Oceans', *Phil. Trans. Roy. Soc., A* 265 : 413–436.

Taylor G.I. (1919) *Phil. Trans. Roy. Soc., A* 220 : 1.

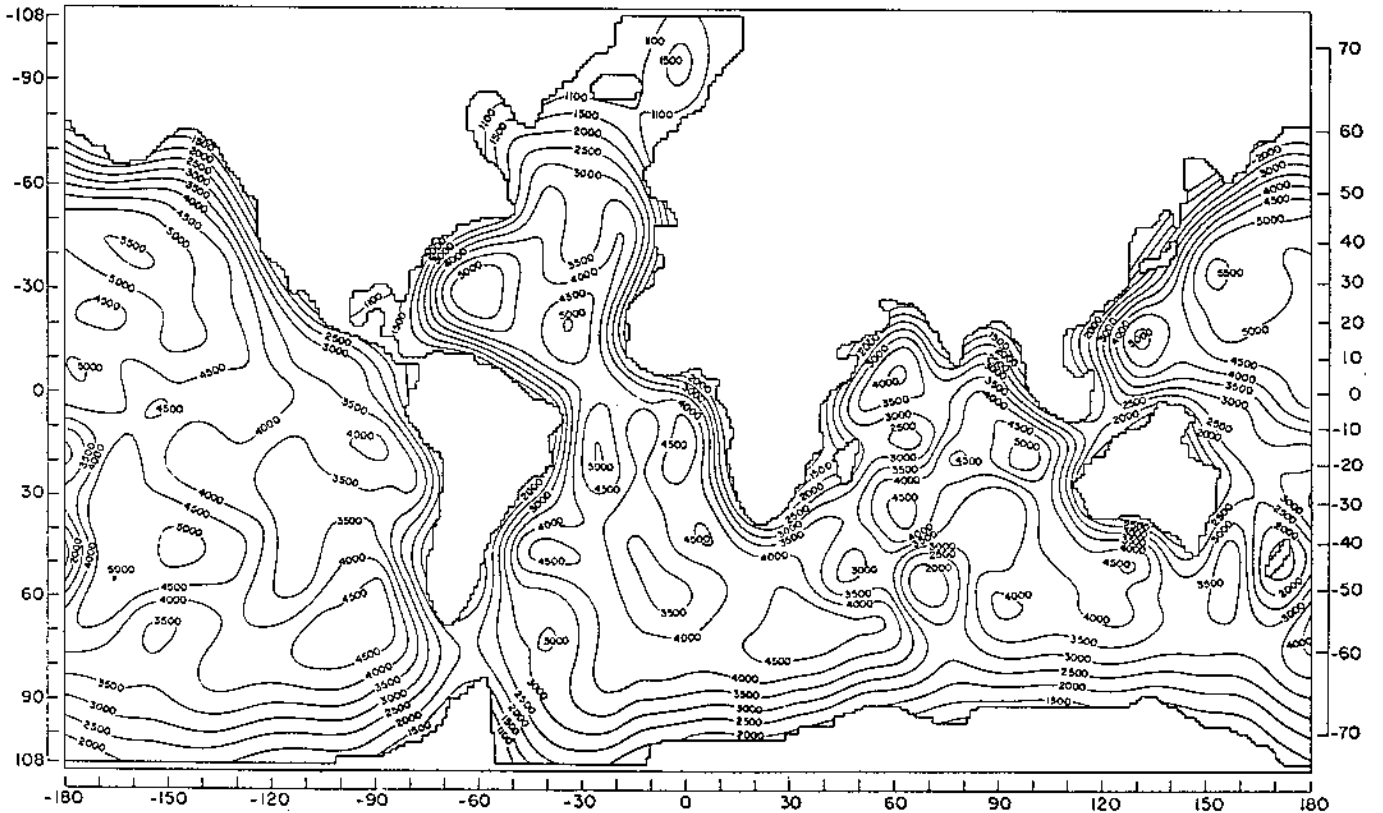

Figure 1 Coastline and ocean depth distributions as used with a 1° grid (Pekeris & Accad 1969).

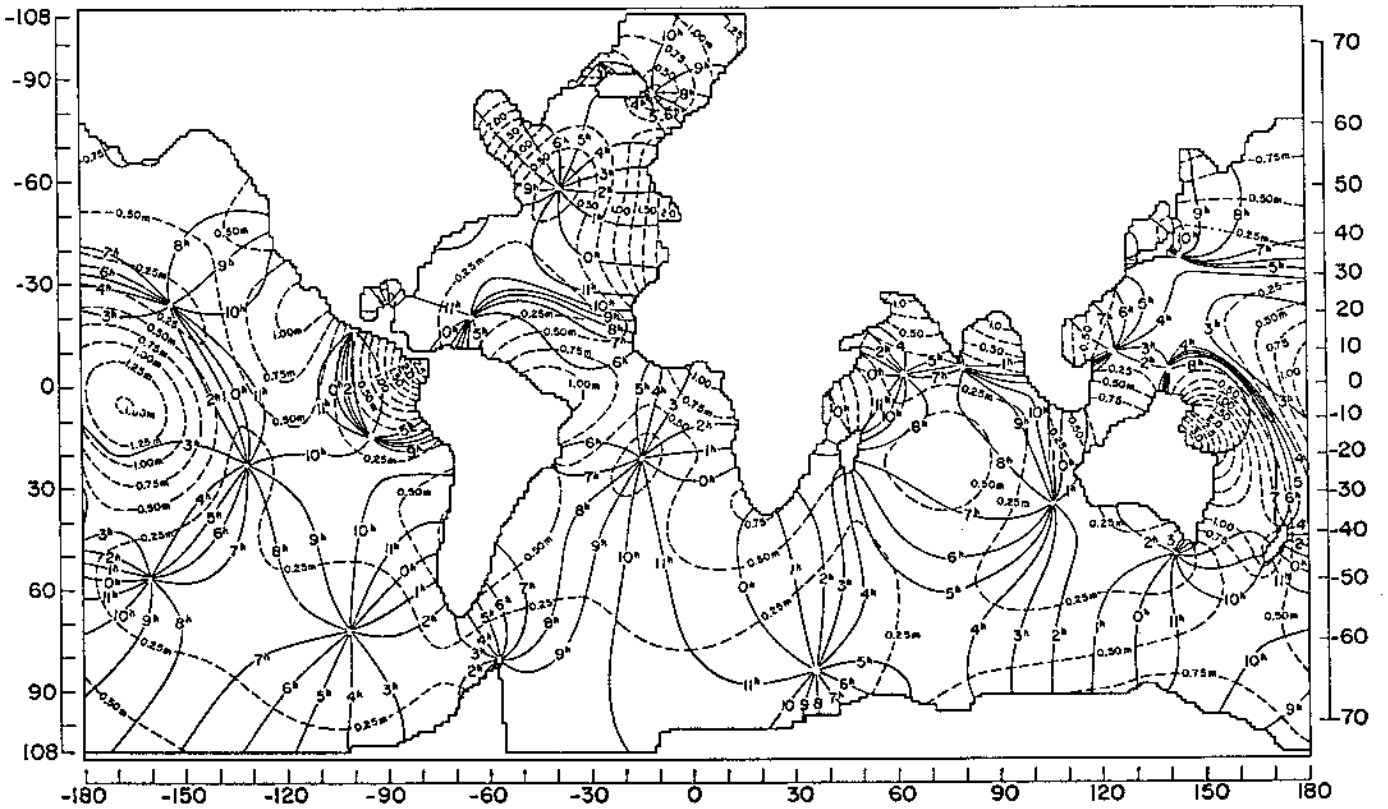

Figure 2 The M_2 tide in the world oceans computed with a 1° grid (Pekeris & Accad 1969). Solid lines = co-tidal lines; broken lines = co-range lines.

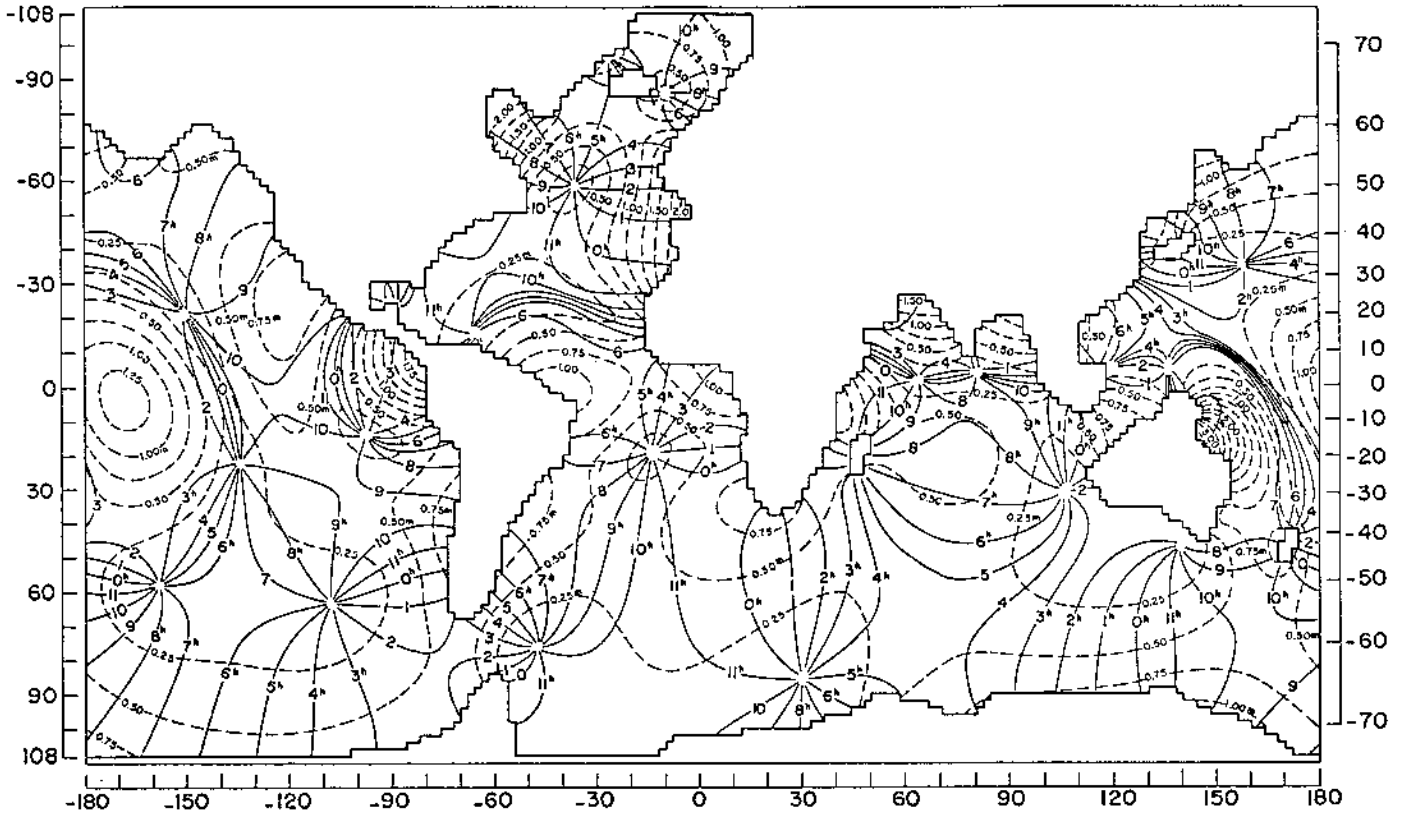

Figure 3 The corresponding M_2 tidal computation with a 2° grid (using a correspondingly coarser coastline distribution).

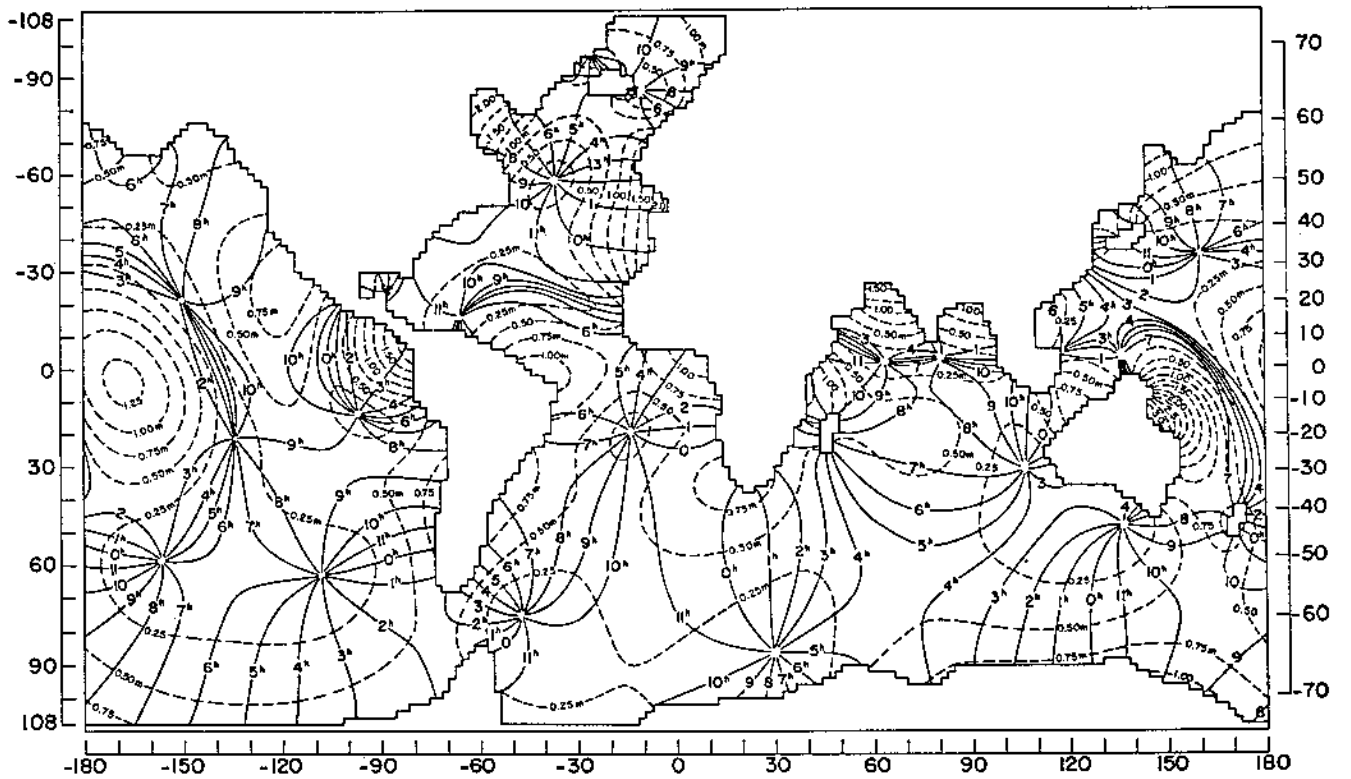

Figure 4 Computation with a 1° grid on the same coastline distribution as in Figure 3.

Figure 5 Comparisons of the tidal computation of Figure 2 with observations of the M_2 tide at islands in the South Atlantic (Pekeris & Accad 1969). Observed phases (in 'hours') are underlined while observed ranges (in cm) are bracketed.

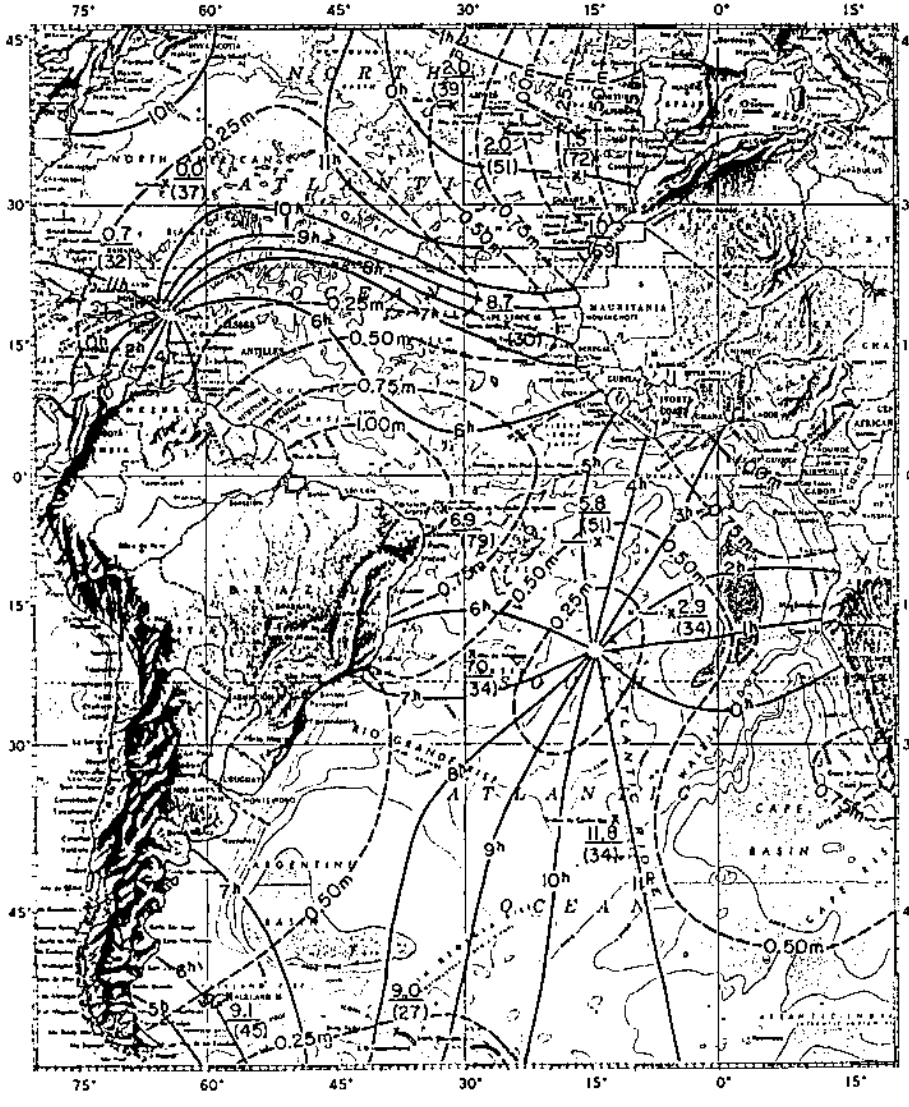

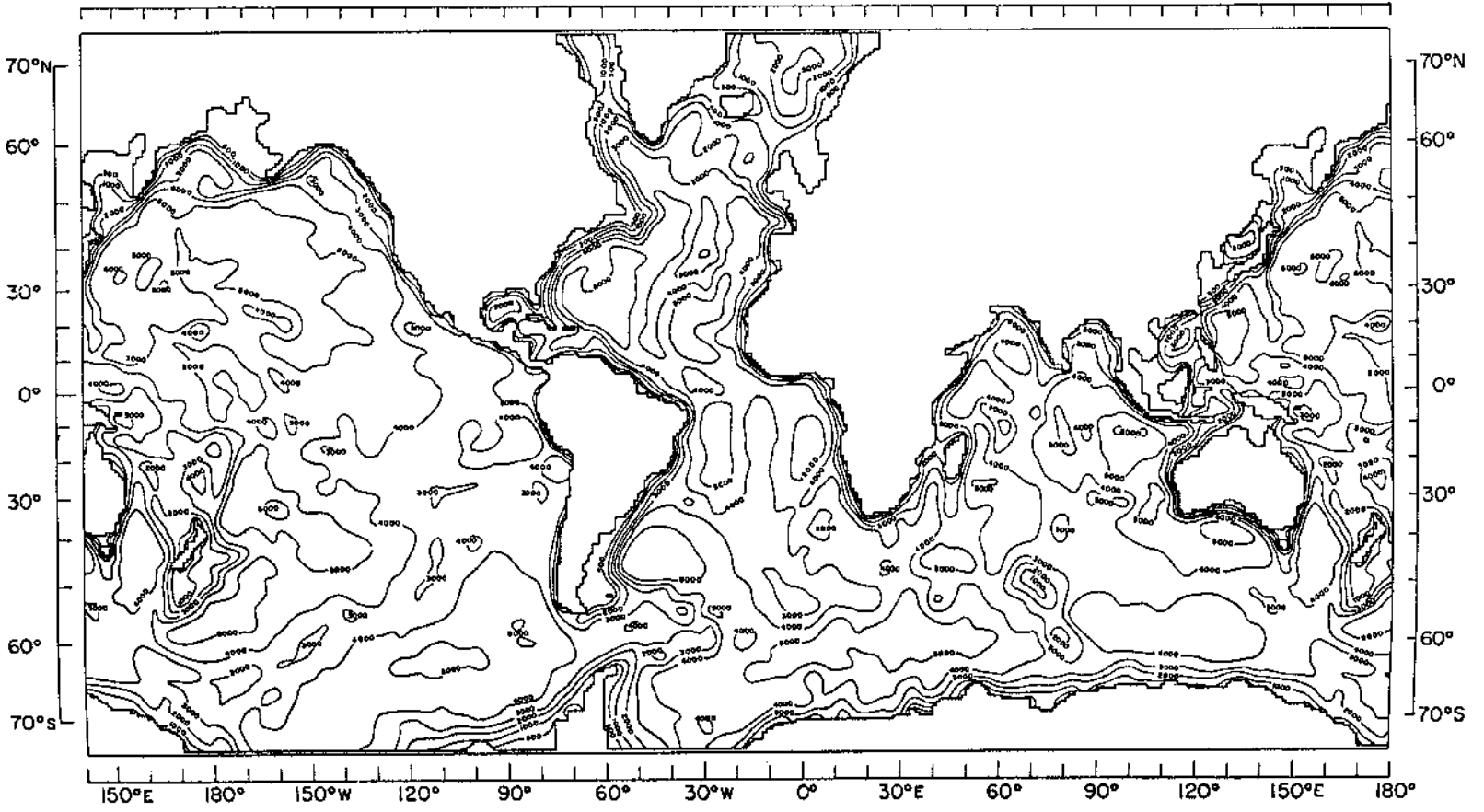

Figure 6 The refined coastline and ocean depth distributions (given here for a 1° grid) that were adopted by Accad & Pekeris (1978).

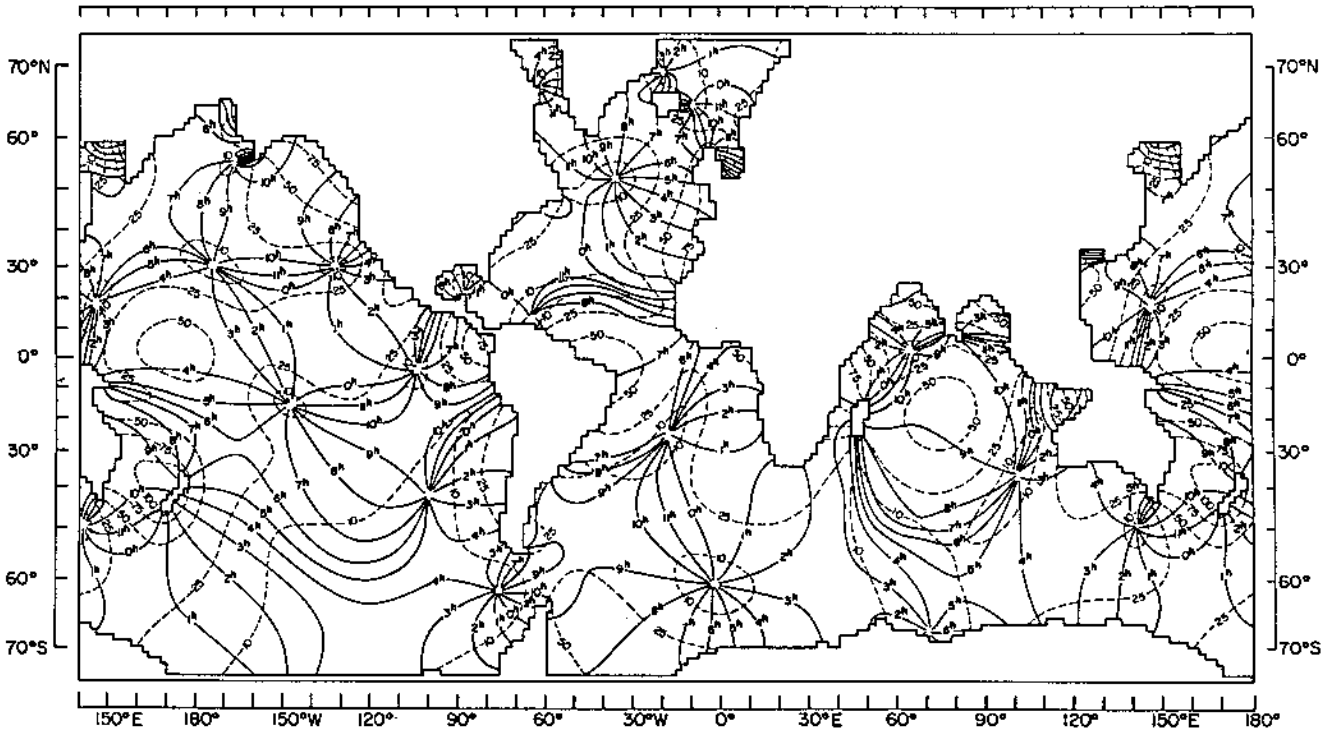

Figure 7 The M_2 tides as computed with a 2° grid (Accad & Pekeris 1978, taking two additional effects into account).

Figure 8 Comparisons of the tidal computation of Figure 7 with observations of the M_2 tide on the Californian coast (Accad & Pekeris 1978). Observed phases (in 'hours') are underlined while observed ranges (in cm) are bracketed.

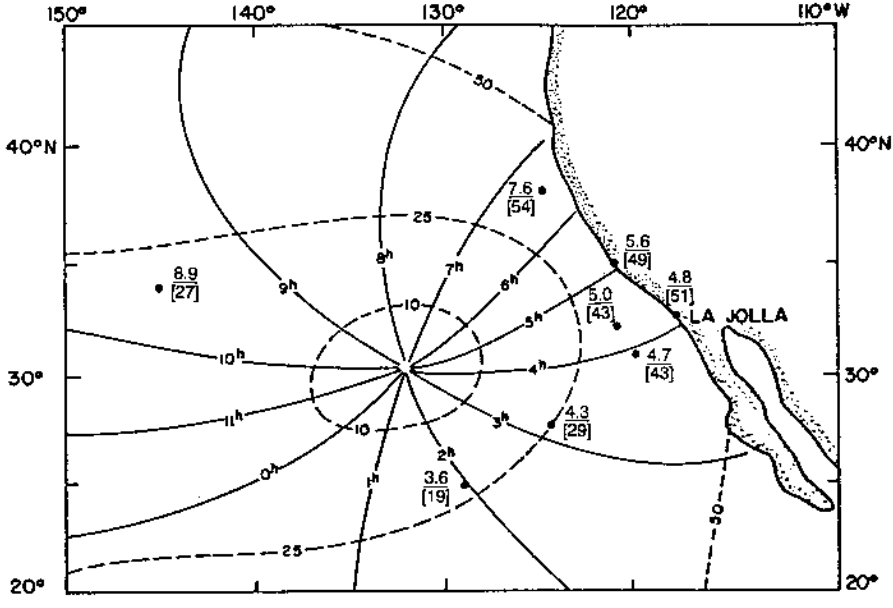

Figure 9 Comparisons of observations (crosses) of tidal phase and range with computed values (circles, connected by line) for the Northeast Pacific coast.

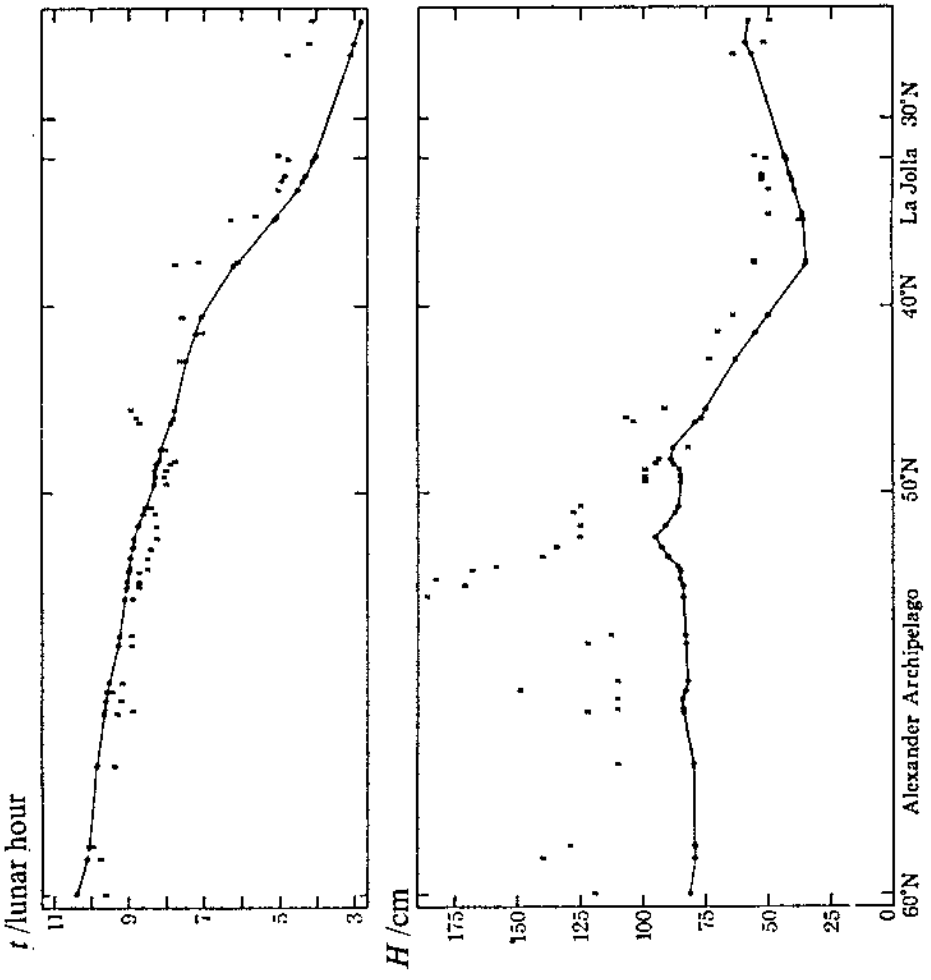

Figure 10 Comparison of observations (crosses) with computed values (circles, connected by line) for the West Atlantic.

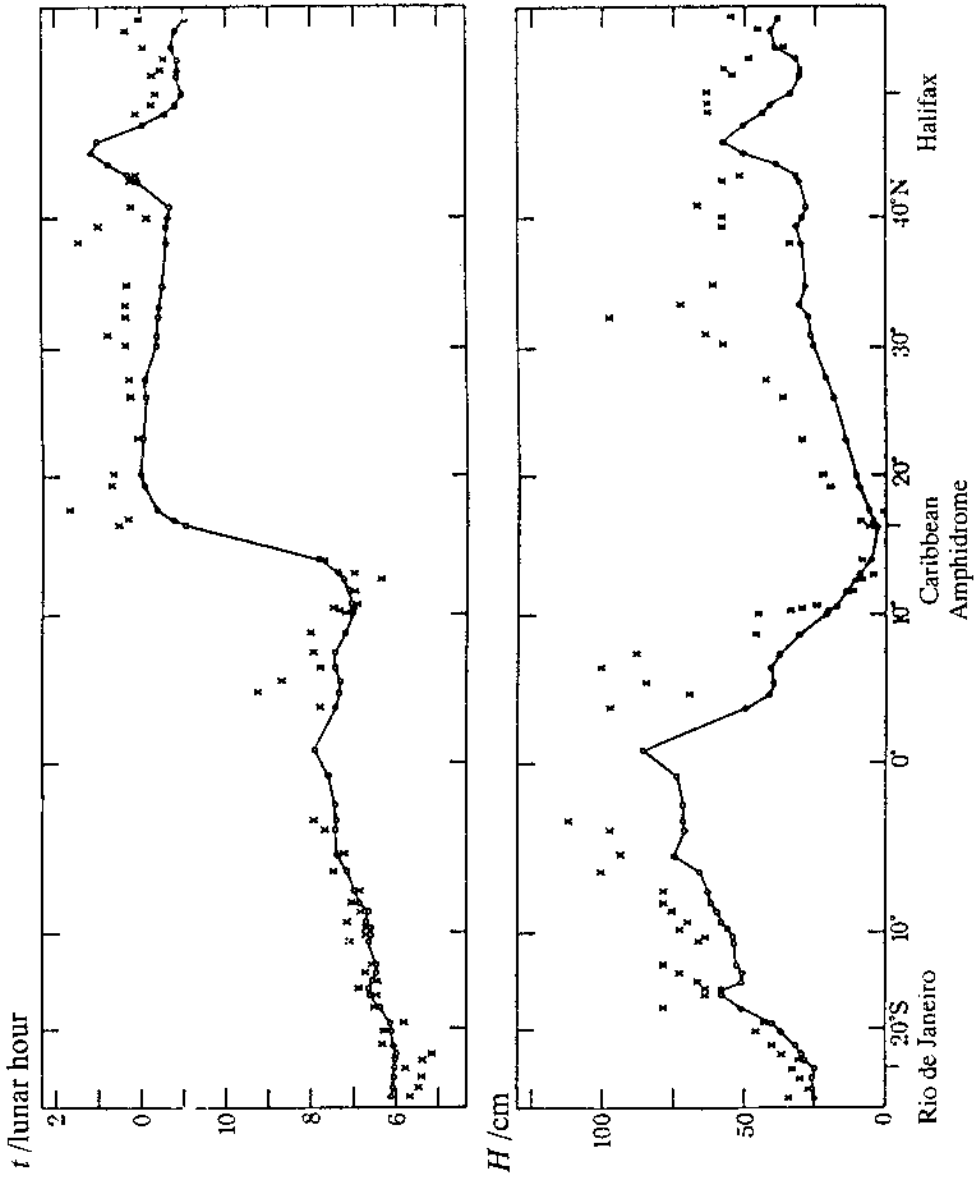

Figure 11 Comparison of observations (crosses) with computed values (circles, connected by line) for the West Pacific.

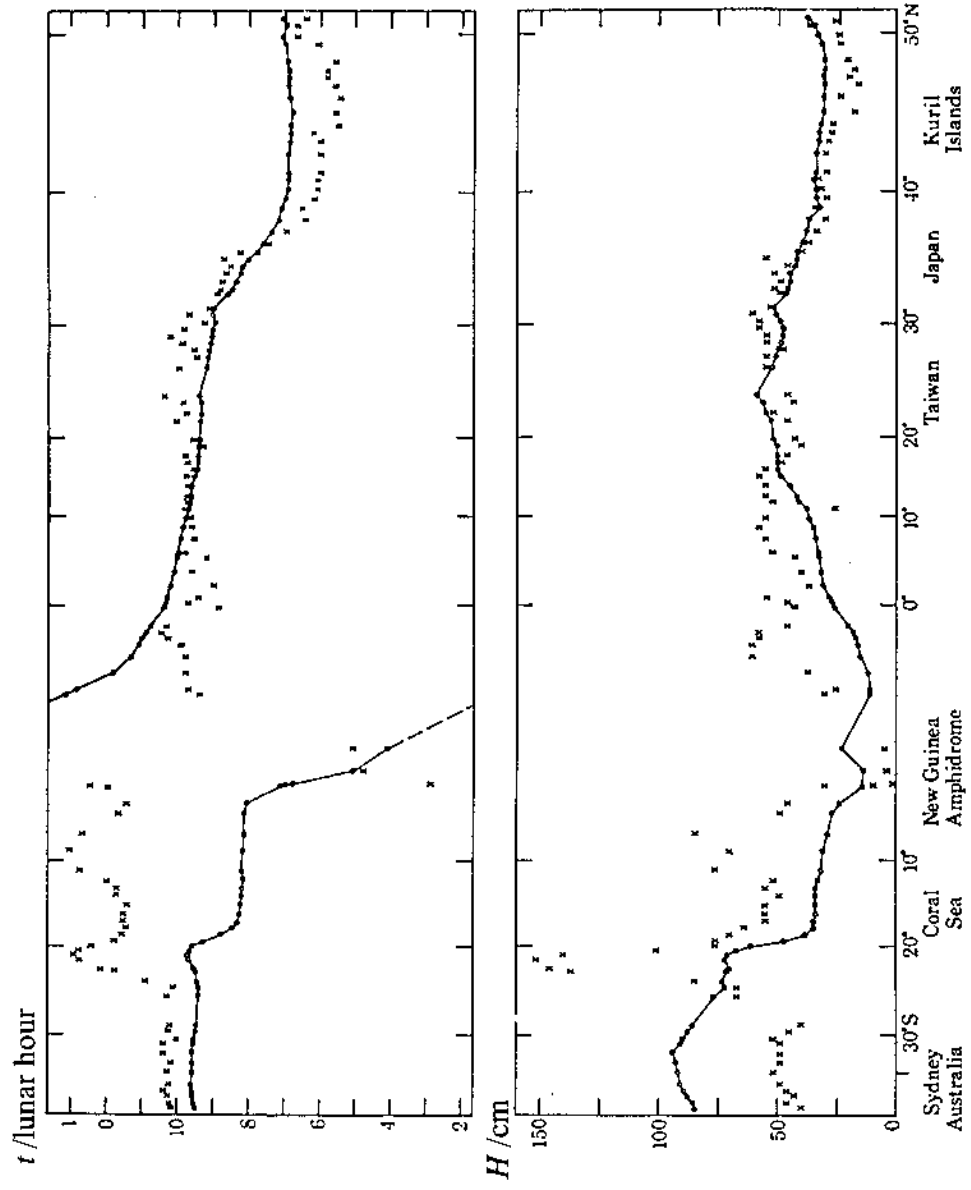

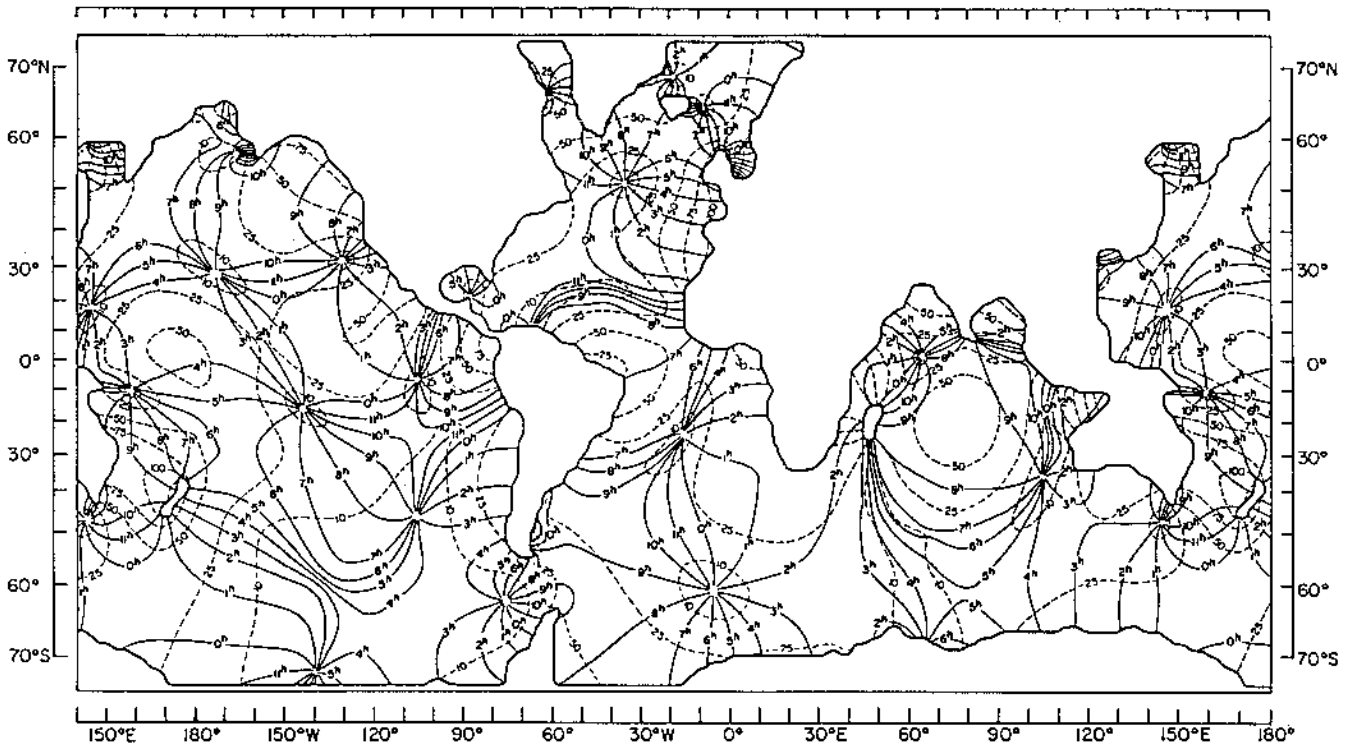

Figure 12 The M_2 tide in the world oceans computed with a 2° grid using a smooth coastline distribution (Accad & Pekeris 1978).